Curvature elasticity of a grafted polyelectrolyte brush

Zhen Lei,[1] Bing Miao,[2] Shuang Yang,[1,*] and Er-Qiang Chen[1,*]

[1]*Beijing National Laboratory for Molecular Sciences, Key Laboratory of Polymer Chemistry and Physics of Ministry of Education, College of Chemistry, Peking University, Beijing 100871, China*

[2]*College of Materials Science and Opto-Electronic Technology, University of Chinese Academy of Sciences, Beijing 100049, China*

(Received 18 March 2015; published 29 June 2015; corrected 1 July 2015)

The curvature elasticity of a polyelectrolyte brush monolayer attached to curved surface is investigated theoretically. An analytical method based on the strong-stretching theory for a Gaussian chain is developed to calculate the elastic modulus induced by a polyelectrolyte brush. In particular, the scaling relations for the bending or Gaussian modulus with respect to system parameters related to the electrostatic interaction (degree of ionization and salt concentration) are derived. Using the numerical self-consistent-field theory, the inner structural, free-energy, and elastic moduli are computed for the polyelectrolyte brush with excluded-volume interactions. Compared to the analytical result, the curvature elasticity has a weaker dependence on the system parameters, which is attributed to the linearization for the Poisson-Boltzmann equation in the analytical treatment. Furthermore, our results are compared to the curvature elasticity of a bare charged surface, wherefrom the unique polyelectrolyte brush effect on the surface elasticity is clarified clearly. The scaling relations derived in our paper can serve as a guide to experimental studies on the related systems.

DOI: 10.1103/PhysRevE.91.062602 PACS number(s): 82.35.Rs, 62.20.de

I. INTRODUCTION

Bending rigidity represents one of the most important mechanical properties of an interface or surface (such as a membrane) [1]. It determines the stability or deformation of the membrane, as well as the self-assembly of block copolymer micelles or vesicles. The curvature energy of an interface or surface is given by the Helfrich free energy [2]

$$f = f_0 + \frac{K}{2}(c_1 + c_2 - 2c_0)^2 + \bar{K}c_1c_2, \qquad (1)$$

where f_0 is the free-energy density of a planar surface, c_1 and c_2 are principal curvatures of the surface orthogonal to each other, and c_0 is spontaneous curvature. The bending modulus K and the Gaussian modulus $\bar{K}$ are two parameters characterizing the curvature elasticity: K represents the ability of the membrane's resistance to bending and $\bar{K}$ indicates whether the formation of a saddle point on the membrane is favorable.

Polymer chains are usually densely grafted on the membrane surfaces to achieve certain purposes, while the interactions between chains induce the change of bending rigidity [3–5]. For example, neutral poly(ethylene glycol) chains are grafted onto both sides of a lipid bilayer and stiffen the supporting membrane [6,7]. Another case is the interface consisting of self-assembled diblock copolymer monolayers, which forms a micelle or vesicle in a solution. Shape deformation may be observed when the bending rigidity of the interface is modified [8,9]. Xu *et al.* [10] prepared an amphiphilic diblock copolymer poly(dimethyl methacrylate)-*b*-poly-*N*-isopropylacrylamide (PDMA-*b*-PNIPAM), which forms a core-corona structure in solution. The charged PDMA in a corona is sensitive to *p*H and induces an obvious shape change of the micelle at a certain *p*H value.

The important issue is how a brush (densely grafted polymer layers) affects the curvature elasticity of the surface. Much effort has been put forth to study the bending rigidity induced by a neutral polymer brush [1,11–19]. Milner and Witten [14], followed by Wang and Safran [13], analytically derived the relation between bending rigidity and systematic parameters such as chain length N, grafting density σ, and excluded-volume parameter u_0 based on the strong-stretching theory (SST). By expanding the free-energy density in power of the curvature, they obtained $K \sim N^3\sigma^{7/3}u_0^{4/3}$. Hiergeist and Lipowsky [20] and Zhulina *et al.* [21] separately obtained the same scaling relation but with a different prefactor by using a scaling argument. Szleifer *et al.* [12] developed a molecular mean-field theory, where the equilibrium area per molecule is determined by the lateral pressure from the polymer brush, to calculate the curvature elasticity of monolayers and bilayers of typical surfactant molecules. They applied this method to investigate the stability of a liposome grafted by polyethylene glycol chains [3,22]. Other methods, such as the numerical self-consistent-field lattice approach [23,24], local-density-functional theory [25], and molecular-dynamics simulation [26], were also developed to calculate the elastic properties of a membrane induced by a polymer brush. In our previous work [27] we applied the numerical self-consistent-field theory (SCFT) to calculate the change of the bending modulus induced by a neutral polymer brush monolayer. Our results reveal that it is important to take into account the effect of solvents explicitly when the grafting density is high enough.

In contrast to the comprehensive understanding for the neutral brush system, there are only a few theoretical studies on the curvature elasticity of a charged polymer monolayer. When polymer chains carry charges, the added salt or *p*H value of the solution has a significant influence on the conformation as well as the physical properties of grafted polyelectrolyte chains. The long-range electrostatic interaction and the presence of multiple scales make the situation rather complicated. Previous theoretical studies focused on the equilibrium structure of a quenched polyelectrolyte brush (the number and position of charges on the chain are both fixed). A deep understanding of their properties has been achieved [21,28–41]. However, less

*Corresponding authors: shuangyang@pku.edu.cn and eqchen@pku.edu.cn

is known about the elastic properties of a charged polymer layer. Apparently, the curvature elasticity is dependent on different factors in a complex way. The investigation of a bare charged plane, a similar but simpler system, based on the linear [42–44] or nonlinear [45,46] Poisson-Boltzmann (PB) equation, provides some useful insights. One may be curious how the bending rigidity will be changed when charges are moved from the surface to a soft polymer shell in the vicinity of the surface.

Zhulina *et al.* [21] analyzed the conformation of a polyelectrolyte chain end grafted to convex spherical and cylindrical surfaces by use of a generalized Daoud-Cotton model and a nonlocal approximation model. In their method, the chain conformational entropy was handled with a strong-stretching approximation and the electrostatic contribution from charged brushes was specified under the assumption of the local electroneutrality approximation (the Donnan rule). This assumption considers that the local excess charges from mobile ions inside the brush compensate for the charges from polymer segments. In the limit of small curvature, they expanded the thickness and free energy in powers of the curvature. In fact, the curvature elasticity of the charged polymer brush can be derived from the curvature expansion. The first work about the curvature elasticity of a weak polyelectrolyte brush was reported by Victorov [47], who gave an analytical estimation for the elastic constant of both a swollen polyelectrolyte brush and a membrane formed by charged diblock copolymers and focused on the effects of salinity and pH of the medium. In Victorov's mean-field model, he employed a boxlike brush model and the local electroneutrality approximation. The approximations simplify the problem considerably, but inevitably it can only give a qualitatively rather than quantitatively accurate prediction.

In this paper we calculate the bending moduli induced by a polyelectrolyte brush using both the SST and SCFT. The SST is only applied to a Gaussian chain system so that we can derive the analytical expressions of K and $\bar{K}$. Our method is a direct extension of the classical works of Zhulina *et al.* [33,34], which analytically investigate a charged polymer brush by use of the SST. Without adopting the local electroneutrality approximation, we apply the Debye-Hückel approximation (the linearized PB equation) to deal with the electrostatic interaction and assume the parabolic form for the electric potential when the grafting surface is slightly bent. Since several approximations are involved, the validity of the analytical results obtained is limited. Meanwhile, we apply the numerical SCFT to solve this problem. In this method the excluded-volume interactions of polymer segments are considered explicitly. We only consider the case with a moderate grafting density, so the second virial model is sufficiently accurate to describe the system. The SCFT can offer rather accurate predictions and is applicable in a large parameter space. However, this method requires a great deal of calculation and the physical mechanism behind the results is not clearly elaborated. Therefore, the combination of the SST and SCFT provides a good way to understand the elastic properties of the polyelectrolyte brush monolayer.

To obtain the bending rigidities induced by a tethered polymer monolayer, we calculate the free energy per unit area for a slightly bent brush on cylindrical and spherical surfaces. The free-energy density is then expanded in powers of the curvature (to second order) with respect to the flat case. However, if the curvature of the grafting surface is large, one has to deal with the inwardly or outwardly grafted brush separately due to the different spatial confinement effect [48]. For a cylindrical brush, the curvatures are $c_1 = 1/R$ and $c_2 = 0$ in Eq. (1) and the free energy per unit area is written as

$$f^c = f_0 + \frac{A_c}{R} + \frac{B_c}{R^2}. \tag{2}$$

Similarly, the curvatures are $c_1 = c_2 = 1/R$ in the spherical case and the free energy is given by

$$f^s = f_0 + \frac{A_s}{R} + \frac{B_s}{R^2}. \tag{3}$$

The expressions of the bending modulus and the Gaussian modulus can be deduced from the coefficients of the second-order term in terms of Eq. (1) [27,49]:

$$K = 2B_c, \quad \bar{K} = B_s - 4B_c. \tag{4}$$

The rest of the paper is organized as follows. We introduce the SST to deal with a charged brush consisting of Gaussian chains. We solve the linearized PB equation for planar, cylindrical, and spherical brushes, respectively. Then we derive the analytical expressions for the thickness of the brush as well as the free energy as a power of $1/R$. The moduli are deduced from the expansion coefficients. We apply the continuous SCFT to handle the charged polymer brush with excluded-volume interactions. The free energy is calculated numerically as a function of surface curvature and the moduli are obtained by fitting. The calculated moduli are found to obey some interesting scaling law with respect to the systematic parameters. We compare and discuss the different results from the two methods and then compare them with the case of a pure charged plane. A summary is given at the end of the paper.

II. STRONG-STRETCHING-THEORY TREATMENT

A. Charged polymer brush grafted on a flat surface

In this section our SST method follows Zhulina and Borisov's classical work [33] for the polyelectrolyte brush. The polymer brush is weakly charged (quenched case), where the polymer chain can be treated as a Gaussian chain. The excluded-volume interaction is neglected for the convenience of the analytical treatment, which corresponds to the system in the θ solvent condition. Here n_p polymer chains are uniformly grafted at one end on an impenetrable neutral surface of area A. The grafting area per chain is $s = A/n_p$ and the grafting density is defined as $\sigma = 1/s$. The brush is assumed to be monodisperse with a natural end-to-end distance $R_0 \equiv bN^{1/2}$, where b is the Kuhn segment length and N is the number of segments per chain. Positive charges are loaded on each polymer chain and are smeared uniformly along the polymer backbone. Here α represents the degree of ionization of segments (we call it the charge fraction) and keeps constant for a quenched polyelectrolyte, i.e., the total charge of each chain is $e\alpha N$, where α is assumed to be small so that the electrostatic stiffening effect can be ignored. The polyelectrolyte brush is in contact with a semi-infinite reservoir of monovalent salt solution with concentration c_0. The distributions of segments

and ions are functions of the z coordinate, which is normal to the grafting surface, assuming a rotational symmetry in the (x,y) plane parallel to the grafting surface. Here h_0 is set as the thickness of the planar brush. The segments are distributed in the range $0 \leqslant z \leqslant h_0$.

The free energy per chain is a summation of three parts:

$$F = F_{\text{polymer}} - S_{\text{ion}} + F_{\text{el}}, \tag{5}$$

where F_{polymer} is the contribution from the nonelectrostatic interaction. It includes conformational entropy loss for stretched polymers and the excluded-volume interaction between segments (we neglect this part here). In addition, S_{ion} represents the translational entropy of mobile ions and F_{el} consists of all the electrostatic interactions in the system. Throughout the paper, we set k_BT as the unit of energy. In terms of the SST, F_{polymer} can be written as [50,51]

$$F_{\text{polymer}} = \frac{3}{2b^2}\int_0^{h_0} g(z')dz' \int_0^{z'} E(z,z')dz, \tag{6}$$

where $g(z')$ is the normalized density distribution of free ends. The function $E(z,z') = dz/dn$ characterizes the local stretching at z when the chain end is located at $z'(z' > z)$. Here $E(z,z')$ obeys the normalization condition

$$N = \int_0^{z'} \frac{dz}{E(z,z')}. \tag{7}$$

The density of segments is expressed as

$$\rho_p(z) = \frac{1}{s}\int_z^{h_0} \frac{g(z')}{E(z,z')}dz'. \tag{8}$$

This density should also satisfy the conservation condition

$$s\int_0^{h_0} dz\, \rho_p(z) = N. \tag{9}$$

The translational entropy term of mobile ions S_{ion} can be given in terms of the concentrations of positive and negative ions (c_+ and c_-) by

$$-\frac{S_{\text{ion}}}{s} = \int_0^{\infty} dz\Bigg[c_+ \ln\left(\frac{c_+(z)}{c_0}\right) + c_- \ln\left(\frac{c_-(z)}{c_0}\right) - [c_+(z) + c_-(z) - 2c_0]\Bigg]. \tag{10}$$

The electrostatic free energy F_{el} follows as

$$\frac{F_{\text{el}}}{s} = \frac{1}{2}\int_0^{\infty} dz\, \Psi(z)\rho_e(z) = \frac{1}{8\pi l_B}\int_0^{\infty} dz|\nabla_z\Psi(z)|^2, \tag{11}$$

where $l_B = e^2/\varepsilon k_BT$ is the Bjerrum length specifying the relative strength of the electrostatic interaction to the thermal energy (e is the elementary charge and ε is the dielectric constant of the solution). The dimensionless electrostatic potential $\Psi(z)$ is related to the electrostatic potential $\psi(z)$ in space via $\Psi(z) = e\psi(z)/kT$. Here $\rho_e(z)$ represents the spatial distribution of excess charge

$$\rho_e(z) = \alpha\rho_p(z) + c_+(z) - c_-(z) \tag{12}$$

and $\Psi(z)$ and $\rho_e(z)$ satisfy the Poisson equation

$$\nabla_z^2\Psi(z) = -4\pi l_B\rho_e(z). \tag{13}$$

In order to deduce the equilibrium distributions of segments and mobile ions, one can minimize the free energy F [Eq. (5)] with respect to the unknown functions $g(z)$, $E(z,z')$, $c_+(z)$, and $c_-(z)$. At the same time, the variation method is also applied on both sides of Eq. (13). Considering the constraint conditions of Eqs. (7)–(9), the equilibrium distributions of segments and ions can be derived. The details can be found in the Appendix of Ref. [33]. The only difference between their work and ours is the way the electrostatic interaction is dealt with. In our case the variation is executed by the Poisson equation (13) and Eq. (11) and then the integration by parts is applied with the boundary condition $\partial\Psi/\partial z|_{z=0} = \partial\Psi/\partial z|_{z=\infty} = 0$. One arrives at results similar to Eq. (A20) in Ref. [33]. Thus it is easier to get the equilibrium distributions. For mobile ions we have $c_+(z) = c_0\exp[-\Psi(z)]$ and $c_-(z) = c_0\exp[\Psi(z)]$. With these distributions Eq. (13) becomes the PB equation.

The most important result in the SST derivation is that, due to the specific boundary condition for the chain trajectory of the polymer brush, the external field acting on each polymer chain [here the field is the reduced electrostatic potential $\Psi(z)$] will be a harmonic potential with a parabolic shape

$$\Psi(z) = A - Bz^2, \tag{14}$$

where the coefficient B is determined as $B = 3\pi^2/8b^2N^2\alpha$. To determine the coefficient A, we apply the Debye-Hückel approximation, where the potential is assumed to be rather small ($\Psi \ll 1$), leading to the linearized PB or the Debye-Hückel equation

$$\frac{d^2\Psi(z)}{dz^2} = \begin{cases} -4\pi l_B[\alpha\rho_p(z) - 2c_0\Psi(z)], & 0 \leqslant z \leqslant h_0 \\ 8\pi l_B c_0\Psi(z), & z \geqslant h_0. \end{cases} \tag{15}$$

From Eq. (14) one finds $\partial^2\Psi/\partial z^2|_{z=h_0} = -2B$ in the brush range $0 \leqslant z \leqslant h_0$, therefore, from Eq. (13), the density of excess charge within the brush remains constant $\rho_e(z) = B/2\pi l_B$. We define the effective surface charge density in the brush region as $Q = sh_0B/2\pi l_B$. According to the Gauss theorem, the boundary condition is $\partial\Psi/\partial z|_{z=h_0} = -4\pi l_BQ/s$. For simplicity, we introduce the Debye screening strength as $\kappa^2 = 8\pi l_Bc_0$. For the $z \geqslant h_0$ region, Eq. (15) can be solved easily with the boundary condition at infinity, leading to

$$\Psi(z) = 2B\kappa^{-1}h_0\exp[-\kappa(z - h_0)], \quad z \geqslant h_0. \tag{16}$$

The potential must satisfy the continuous condition at $z = h_0$, i.e., $\Psi(h_0) = A - Bh_0^2$. The coefficient A is therefore determined to be

$$A = 2Bh_0\kappa^{-1} + Bh_0^2. \tag{17}$$

The segment density $\rho_p(z)$ in the range $0 \leqslant z \leqslant h_0$ is also determined from Eq. (15). Until now, the only unknown variable is the brush thickness h_0. It can be solved by using the conservation condition (9),

$$\kappa h_0 + \kappa^2h_0^2 + \frac{\kappa^3h_0^3}{3} = \frac{2\pi l_BN\alpha\kappa}{Bs}. \tag{18}$$

The solution of Eq. (18) reads

$$\kappa h_0 = \left(1 + \frac{6\pi l_BN\alpha\kappa}{Bs}\right)^{1/3} - 1. \tag{19}$$

When $\kappa h_0 \gg 1$, Eq. (19) can be simplified as

$$h_0 = \left(\frac{16 l_B b^2}{\pi}\right)^{1/3} N\alpha^{2/3}\sigma^{1/3}\kappa^{-2/3}. \tag{20}$$

The scaling relation in Eq. (20) is consistent with Pincus's strong-screening limit [28]. In general cases, the salt concentration is not so low and the brush thickness for long chains is much larger than $1/\kappa$. The condition $\kappa h_0 \gg 1$ always holds.

B. Polyelectrolyte brush grafted on a cylindrical surface

To calculate the elastic moduli, we now consider the charged polymer brush grafted onto the outward surface of a cylinder with a large radius R. Similarly, all the variables are only dependent on the radial coordinate r due to the rotational symmetry. The coordinate r is related to the normal distance x to the surface via $r = R + x$. The brush thickness becomes h after bending. The free-energy expressions of each term become

$$F_{\text{polymer}} = \frac{3}{2b^2}\int_R^{R+h_0} g(r')\left(\frac{r'}{R}\right)dr' \int_R^{r'} E(r,r')dr, \tag{21a}$$

$$-\frac{S_{\text{ion}}}{s} = \int_R^{R+\infty} dr\left(\frac{r}{R}\right)\left[c_+ \ln\left(\frac{c_+(r)}{c_0}\right) + c_- \ln\left(\frac{c_-(r)}{c_0}\right) - [c_+(r) + c_-(r) - 2c_0]\right], \tag{21b}$$

$$\frac{F_{\text{el}}}{s} = \frac{1}{2}\int_R^{R+\infty} dr\left(\frac{r}{R}\right)\Psi(r)\rho_e(r) = \frac{1}{8\pi l_B}\int_R^{R+\infty} dr\left(\frac{r}{R}\right)|\nabla_r \Psi(r)|^2. \tag{21c}$$

Since the surface is bent slightly, we still assume that the distribution of the reduced electrostatic potential is parabolic

$$\Psi(r) = A_1 - Bx^2. \tag{22}$$

The expression of coefficient B is the same as in the planar case and the coefficient A_1 needs to be determined. For a cylindrical brush the conservation condition becomes

$$s\int_R^{R+h} \rho_p(z)\frac{r}{R}dr = N. \tag{23}$$

The linearized PB equation is written as

$$\frac{\partial^2\Psi(r)}{\partial r^2} + \frac{1}{r}\frac{\partial\Psi(r)}{\partial r} = \begin{cases} -4\pi l_B[\alpha\rho_p(r) - 2c_0\Psi(r)], & R \leqslant r \leqslant R+h \\ 8\pi l_B c_0\Psi(r), & r \geqslant R+h. \end{cases} \tag{24}$$

Using the boundary condition that the potential is zero at an infinite distance, the above equation can be solved in the range $r \geqslant R + h$ and the solution reads

$$\Psi(r) = 4\pi l_B \frac{\sigma_e}{\kappa}\frac{K_0[\kappa r]}{K_1[\kappa(R+h)]}, \tag{25}$$

where K_0 and K_1 are the modified Bessel functions of zeroth and *1*th order, respectively, and σ_e is the effective surface charge density of the cylindrical brush layer (in units of elementary charge). It corresponds to the integral over the distribution of excess charge in the range $R \leqslant r \leqslant R + h$,

$$\sigma_e = \int_R^{R+h} \rho_e(r)\frac{r}{R}dr = \frac{4c_0 B}{\kappa^2}\left(h + \frac{h^2}{R}\right). \tag{26}$$

The coefficient A_1 is determined in terms of the continuity condition of $\Psi(r)$ at the edge of the brush $r = R + h$,

$$A_1 = Bh^2 + 4\pi l_B \frac{\sigma_e}{\kappa}\frac{K_0[\kappa(R+h)]}{K_1[\kappa(R+h)]}. \tag{27}$$

Applying the series expansion of Bessel functions

$$\lim_{z\to\infty} K_0(z) = \sqrt{\frac{\pi}{2z}}e^{-z}\left[1 - \frac{1}{8z} + \frac{9}{128z^2} + \cdots\right],$$

$$\lim_{z\to\infty} K_1(z) = \sqrt{\frac{\pi}{2z}}e^{-z}\left[1 + \frac{3}{8z} - \frac{15}{128z^2} + \cdots\right],$$

Eq. (27) can be expanded to the second order of $1/R$. The coefficient A_1 can be written as

$$\frac{A_1}{B} = h^2 + \frac{2h}{\kappa}\left[1 + \frac{1}{R}\left(h - \frac{1}{2\kappa}\right) + \frac{1}{R^2}\frac{15}{64\kappa^2}\right]. \tag{28}$$

The conservation condition (23) leads to the equation for the brush thickness h,

$$A_1 h + \frac{A_1}{2R}h^2 - \frac{B}{3}h^3 - \frac{B}{4R}h^4 + \frac{2B}{\kappa^2}\left(h + \frac{h^2}{R}\right) = \frac{N}{s}\frac{\alpha}{2c_0}. \tag{29}$$

To proceed we seek a series solution for Eq. (29) and expand the brush thickness h to the second order of $1/R$,

$$h = h_0 + h_1\frac{1}{R} + h_2\frac{1}{R^2}, \tag{30}$$

where h_0 is the brush thickness for a flat surface. Upon substituting Eqs. (28) and (30), Eq. (29) is expanded as a power series of $1/R$. The zeroth-order term gives the equation for the planar brush thickness h_0 [Eq. (18)]. Applying the requirement that both the first- and second-order terms must

be zero, we find

$$h_1 = \frac{-4h_0^2 - 12\kappa h_0^3 - \kappa^2 h_0^4}{8(1+\kappa h_0)^2}, \tag{31a}$$

$$h_2 = \frac{\left[-(15/64)h_0^2 + (\kappa/4)h_0^3 - (\kappa^2/2)h_0^4\right] - \left[\kappa h_0 + (9\kappa^2/2)h_0^2 + (\kappa^3/2)h_0^3\right]h_1 - (\kappa^2 + \kappa^3 h_0)h_1^2}{\kappa + 2\kappa^2 h_0 + \kappa^3 h_0^2}. \tag{31b}$$

It is assumed that during the tiny bending process of the surface ($R \gg 1$), the change of free energy per unit area mainly comes from the electrostatic interaction and the translational entropy of mobile ions, while the stretching energy remains almost constant with changing R (the variation of conformational entropy is rather small). Using the Debye-Hückel approximation and ignoring the stretching energy, the free energy per unit area f^c of a cylindrical brush is given by

$$f^c = \frac{F}{s} \approx \frac{1}{2}\int_R^{R+h_1} \alpha\rho_p(r)\Psi(r)\frac{r}{R}\,dr. \tag{32}$$

Here f^c is also expanded to the second order of $1/R$ as

$$f^c = f_0 + f_1^c\frac{1}{R} + f_2^c\frac{1}{R^2}. \tag{33}$$

After straightforward algebra, one arrives at the final expression of f^c with the zeroth-order term

$$\frac{f_0}{c_0B^2} = \frac{4}{\kappa^3}h_0^2 + \frac{16}{3\kappa^2}h_0^3 + \frac{8}{3\kappa}h_0^4 + \frac{8}{15}h_0^5, \tag{34}$$

which is exactly the result for the planar case. The expression of the second-order term is

$$\begin{aligned}\frac{f_2^c}{c_0B^2} = {} & h_0{}^5h_1 + \frac{16}{3}h_0^3h_1^2 + \frac{8}{3}h_0^4h_2^2 + \frac{15}{16\kappa^5}h_0^2 + \frac{7}{8\kappa^4}h_0^3 - \frac{4}{\kappa^4}h_0h_1 - \frac{11}{8\kappa^3}h_0^4 + \frac{12}{\kappa^3}h_0^2h_1 + \frac{4}{\kappa^3}h_1^2 \\ & + \frac{8}{\kappa^3}h_0h_2 + \frac{15}{2\kappa^2}h_0^5 + \frac{116}{3\kappa^2}h_0^3h_1 + \frac{16}{\kappa^2}h_0h_1^2 + \frac{16}{\kappa^2}h_0^2h_2 + \frac{1}{\kappa}h_0^6 + \frac{55}{3\kappa}h_0^4h_1 + \frac{16}{\kappa}h_0^2h_1^2 + \frac{32}{3\kappa}h_0^3h_2.\end{aligned} \tag{35}$$

When $\kappa h_0 \gg 1$, Eq. (31) can be simplified as

$$h_1 = -\frac{h_0^2}{8}, \quad h_2 = \frac{3h_0^3}{64}. \tag{36}$$

The second-order term is then simplified to

$$f_2^c = c_0B^2\frac{h_0^7}{12}. \tag{37}$$

With the solution in the cylindrical coordinates, the bending modulus induced by a charged brush is obtained from Eq. (4) as

$$K = \frac{c_0B^2}{6}h_0^7 = 3\times 2^{-14/3}\left(\frac{b}{\pi}\right)^{2/3}N^3\alpha^{8/3}\sigma^{7/3}c_0^{-4/3}. \tag{38}$$

C. Polyelectrolyte brush grafted on a spherical surface

We further consider a slightly bent polyelectrolyte brush grafted on a spherical outward surface of radius R. All the variables depend only on the radial coordinate r, which is related to the normal distance x to the surface via $r = R + x$. The brush thickness is h. The free-energy expressions is given by

$$F_{\text{polymer}} = \frac{3}{2b^2}\int_R^{R+h_0} g(r')\left(\frac{r'}{R}\right)^2 dr'\int_R^{r'} E(r,r')dr, \tag{39a}$$

$$-\frac{S_{\text{ion}}}{s} = \int_R^{R+\infty} dr\left(\frac{r}{R}\right)^2\left[c_+\ln\left(\frac{c_+(r)}{c_0}\right) + c_-\ln\left(\frac{c_-(r)}{c_0}\right) - [c_+(r) + c_-(r) - 2c_0]\right], \tag{39b}$$

$$\frac{F_{\text{el}}}{sk_BT} = \frac{1}{2}\int_R^{R+\infty} dr\left(\frac{r}{R}\right)^2\Psi(r)\rho_e(r) = \frac{1}{8\pi l_B}\int_R^{R+\infty} dr\left(\frac{r}{R}\right)^2|\nabla_r\Psi(r)|^2. \tag{39c}$$

The conservation condition in spherical coordinates becomes

$$s\int_R^{R+h}\rho_p(z)\left(\frac{r}{R}\right)^2 dr = N. \tag{40}$$

The reduced electrostatic potential is assumed to be a parabolic form

$$\Psi(r) = A_2 - Bx^2. \tag{41}$$

The linearized PB equation now is given by

$$\frac{\partial^2\Psi(r)}{\partial r^2} + \frac{2}{r}\frac{\partial\Psi(r)}{\partial r} = \begin{cases} -4\pi l_B[\alpha\rho_p(r) - 2c_0\Psi(r)], & R \leqslant r \leqslant R+h \\ 8\pi l_B c_0\Psi(r), & r \geqslant R+h. \end{cases} \tag{42}$$

The solution to Eq. (42) in the range $r \geqslant R+h$ follows as

$$\Psi(r) = 4\pi l_B\sigma_e\frac{R+h}{1+\kappa(R+h)}, \tag{43}$$

where the surface charge density σ_e is obtained as

$$\sigma_e = \frac{4c_0B}{\kappa^2}\left(h + 2\frac{h^2}{R} + \frac{h^3}{R^2}\right). \tag{44}$$

According to the continuity condition $\Psi(r)$ at $r = R+h$, one can obtain the coefficient A_2 in the form

$$A_2 = Bh^2 + 4\pi l_B\sigma_e\frac{R+h}{1+\kappa(R+h)}. \tag{45}$$

Equation (45) can be expanded as a power series of $1/R$ with substitution of Eq. (44). To second order the result reads

$$\frac{A_2}{B} = h^2 + \frac{2h}{\kappa}\left[1 + \frac{1}{R}\left(2h - \frac{1}{\kappa}\right) + \frac{1}{R^2}\left(h^2 - \frac{h}{\kappa} + \frac{1}{\kappa^2}\right)\right]. \tag{46}$$

In terms of the conservation condition in Eq. (40), the equation for the brush thickness is obtained as

$$\frac{A_2}{R^2}\left(R^2h + Rh^2 + \frac{h^3}{3}\right) - \frac{B}{R^2}\left(\frac{R^2h^3}{3} + \frac{Rh^4}{2} + \frac{h^5}{5}\right) + \frac{2B}{\kappa^2R^2}(R^2h + 2Rh^2 + h^3) = \frac{N}{s}\frac{\alpha}{2c_0}. \tag{47}$$

Expanding h to the second order of $1/R$ gives

$$h = h_0 + h_1\frac{1}{R} + h_2\frac{1}{R^2}. \tag{48}$$

Substituting Eq. (48) into Eq. (47), we have

$$h_1 = \frac{-4h_0^2 - 12\kappa h_0^3 - \kappa^2h_0^4}{4(1+\kappa h_0)^2}, \tag{49a}$$

$$h_2 = \frac{-5h_0^2 + 5\kappa h_0^3 - 10h_0h_1\kappa - 20h_0^4\kappa^2 - 45h_0^2h_1\kappa^2 - 5h_1^2\kappa^2 - 2h_0^5\kappa^3 - 5h_0^3h_1\kappa^3 - 5h_0h_1^2\kappa^3}{5\kappa(1+h_0\kappa)^2}. \tag{49b}$$

Ignoring the stretching energy of polymer chains, the free energy per unit area f^s can be written as

$$f^s = \frac{F}{s} \approx \frac{1}{2}\int_R^{R+h_1}\alpha\rho_p(r)\Psi(r)\left(\frac{r}{R}\right)^2 dr. \tag{50}$$

This expression is expanded to the second order of $1/R$; after some algebra we have

$$f^s = f_0 + f_1^s\frac{1}{R} + f_2^s\frac{1}{R^2}. \tag{51}$$

The zeroth-order term is the free-energy density in planar case and the second-order term reads

$$\begin{aligned}\frac{f_2^s}{c_0B^2} = {} & \frac{8}{105}h_0^7 + 2h_0^5h_1 + \frac{16}{3}h_0^3h_1^2 + \frac{8}{3}h_0^4h_2 + \frac{4h_0^2}{\kappa^5} - \frac{8h_0h_1}{\kappa^4} - \frac{16}{3}\frac{h_0^4}{\kappa^3} + \frac{24h_0^2h_1}{\kappa^3} + \frac{4h_1^2}{\kappa^3} + \frac{8h_0h_2}{\kappa^3} \\ & + \frac{562h_0^5}{15\kappa^2} + \frac{232h_0^3h_1}{3\kappa^2} + \frac{16h_0h_1^2}{\kappa^2} + \frac{16h_0^2h_2}{\kappa^2} + \frac{36h_0^6}{5\kappa} + \frac{110h_0^4h_1}{3\kappa} + \frac{16h_0^2h_1^2}{\kappa} + \frac{32h_0^3h_2}{3\kappa},\end{aligned} \tag{52}$$

When $\kappa h_0 \gg 1$, Eq. (49) is simplified as

$$h_1 = -\frac{h_0^2}{4}, \quad h_2 = -\frac{17h_0^3}{80}. \tag{53}$$

The second-order term of the free-energy density is given by

$$f_2^s = -c_0 B^2 \frac{23 h_0^7}{35}. \tag{54}$$

Based on Eqs. (4), (37), and (54), the Gaussian modulus induced by the polyelectrolyte brush is obtained in the form

$$\overline{K} = f_2^s - 4 f_2^c = c_0 B^2 \left(-\frac{104}{105} h_0^7\right) = -\frac{624}{35} \times 2^{-14/3} \left(\frac{b}{\pi}\right)^{2/3} N^3 \alpha^{8/3} \sigma^{7/3} c_0^{-4/3}. \tag{55}$$

III. SELF-CONSISTENT-FIELD THEORY

A. The SCFT for a polyelectrolyte brush

In this section we perform the SCFT calculation to investigate the curvature elasticity. The SCFT is based on Edward's Gaussian chain model. The short-range many-body interaction between polymer segments is considered, which is represented by the excluded-volume parameter u_0. When $u_0 = 0$, the system is equal to that we treated in the SST. Within the framework of the SCFT, the segment density is defined as

$$\widehat{\rho}(\mathbf{r}) = \sum_{\alpha=1}^{n} \int_0^N \delta[\mathbf{r} - \mathbf{r}_\alpha(t)] dt, \tag{56}$$

where t represents the contour length variable along the polymer backbone and varies from 0 at the grafted end to N at the free end. The space curve $\mathbf{r}_\alpha(t)$ denotes the configuration of the αth chain. The Hamiltonian of the system is expressed as

$$H = \frac{3}{2b^2} \sum_{i=1} \int_0^N dt \left(\frac{\partial \mathbf{R}_i}{\partial t}\right)^2 + \frac{u_0}{2} \int d\mathbf{r} \hat{\rho} p_p^2(\mathbf{r}) + \int d\mathbf{r} \left[\hat{\rho}_e(\mathbf{r}) \phi(\mathbf{r}) - \frac{1}{8\pi l_B} |\nabla \phi(\mathbf{r})|^2\right]. \tag{57}$$

The first term is the conformational entropy of the polymer chains. The second term gives the excluded-volume interaction, and the third term describes the electrostatic interaction. Then the partition function of the system follows as

$$Z = \prod_i D\{\mathbf{R}_i(t)\} \prod_j \mathbf{r}_j \exp(-H). \tag{58}$$

In the SCFT, all interactions are replaced by an effective field. The statistics of the system is reduced to a single-chain problem in the effective field $w(\mathbf{r}) = w_p(\mathbf{r}) + w_e(\mathbf{r})$, where $w_p(\mathbf{r})$ and $w_e(\mathbf{r})$ originate from the excluded-volume interaction and the electrostatic interaction, respectively. They are related to the ensemble-average segment density $\rho_p(\mathbf{r})$ and reduced electrostatic potential $\Psi(\mathbf{r}) = e\phi(\mathbf{r})/k_B T$ as

$$w_p(\mathbf{r}) = u_0 \rho_p(\mathbf{r}), \quad w_e(\mathbf{r}) = \Psi(\mathbf{r}). \tag{59}$$

The segment density satisfies the conservation condition

$$\int_V d\mathbf{r}\, \rho_p(\mathbf{r}) = NA\sigma. \tag{60}$$

The concentrations of positive and negative mobile ions are given by the Boltzmann distributions

$$c_+(\mathbf{r}) = c_0 \exp[-\Psi(\mathbf{r})], \quad c_-(\mathbf{r}) = c_0 \exp[\Psi(\mathbf{r})], \tag{61}$$

where c_0 is the salt concentration in bulk solution. The average charge density at any point $\mathbf{r}$ follows as

$$\rho_e(\mathbf{r}) = \alpha \rho_p(\mathbf{r}) + c_+(\mathbf{r}) - c_-(\mathbf{r}). \tag{62}$$

Combining with the distribution of mobile ions, the PB equation of the system is given by

$$\nabla^2 \Psi(\mathbf{r}) = -4\pi l_B \rho_e(\mathbf{r}). \tag{63}$$

The central quantity is the chain propagator G. It represents the probability of finding a chain of length t with its ends fixed at $\mathbf{r}_\alpha(0) = \mathbf{r}'$ and $\mathbf{r}_\alpha(t) = \mathbf{r}$ under the mean field $w(\mathbf{r})$. It is given by

$$G(\mathbf{r},t;\mathbf{r}') = \int_{\mathbf{r}(0)=\mathbf{r}'}^{\mathbf{r}(t)=\mathbf{r}} D[\mathbf{r}_\alpha(\cdot)] \times \exp\left\{-\int_0^N \left[\frac{3}{2b^2} \dot{\mathbf{r}}_\alpha^2(t) + w[\mathbf{r}_\alpha(t)]\right] dt\right\}. \tag{64}$$

One has to solve G from the diffusion equation

$$\frac{\partial}{\partial t} G(\mathbf{r},t;\mathbf{r}') = \left[\frac{b^2}{6} \nabla^2 - w(\mathbf{r})\right] G(\mathbf{r},t;\mathbf{r}'). \tag{65}$$

The initial condition of G is $G(\mathbf{r},0;\mathbf{r}') = \delta(\mathbf{r} - \mathbf{r}')$. The boundary condition is $G(\mathbf{r},t;\mathbf{r}') = 0$ with $\mathbf{r}$ or $\mathbf{r}'$ is on the surface. With the given propagator, the average segment density can be obtained by

$$\rho(\mathbf{r}) = \frac{\sigma A}{V Q} \int_0^N \int d\mathbf{r}'' G(\mathbf{r},t;\mathbf{r}_0) G(\mathbf{r}'', N-t;\mathbf{r}) dt, \tag{66}$$

where $\mathbf{r}_0$ represents the position of the grafting point on the surface. The partition function of a single chain satisfies

$$Q = \frac{1}{V} \int_V G(\mathbf{r},N;\mathbf{r}_0) d\mathbf{r}. \tag{67}$$

The free energy of the system can be written as

$$F = -\frac{1}{2} \int_V d\mathbf{r}\, \Psi(\mathbf{r}) \rho_e(\mathbf{r}) - \frac{u_0}{2} \int_V d\mathbf{r}\, \rho_p(\mathbf{r})^2 - \int_V d\mathbf{r} [c_+(\mathbf{r}) + c_-(\mathbf{r}) - 2c_0] - \sigma \ln Q. \tag{68}$$

Equations (59)–(63) and (65)–(67) consist of a set of self-consistent equations. We need to solve them numerically in planar, cylindrical, and spherical coordinates to obtain the equilibrium distributions of fields, segments, and mobile ions. We use a relaxation iteration method to solve the SCFT equations (see our previous work for details [27]). Since the electrostatic interaction in low salt concentration extends far from the surface, we need a large box to solve the problem precisely. Therefore, a nonuniform grid is needed to speed up

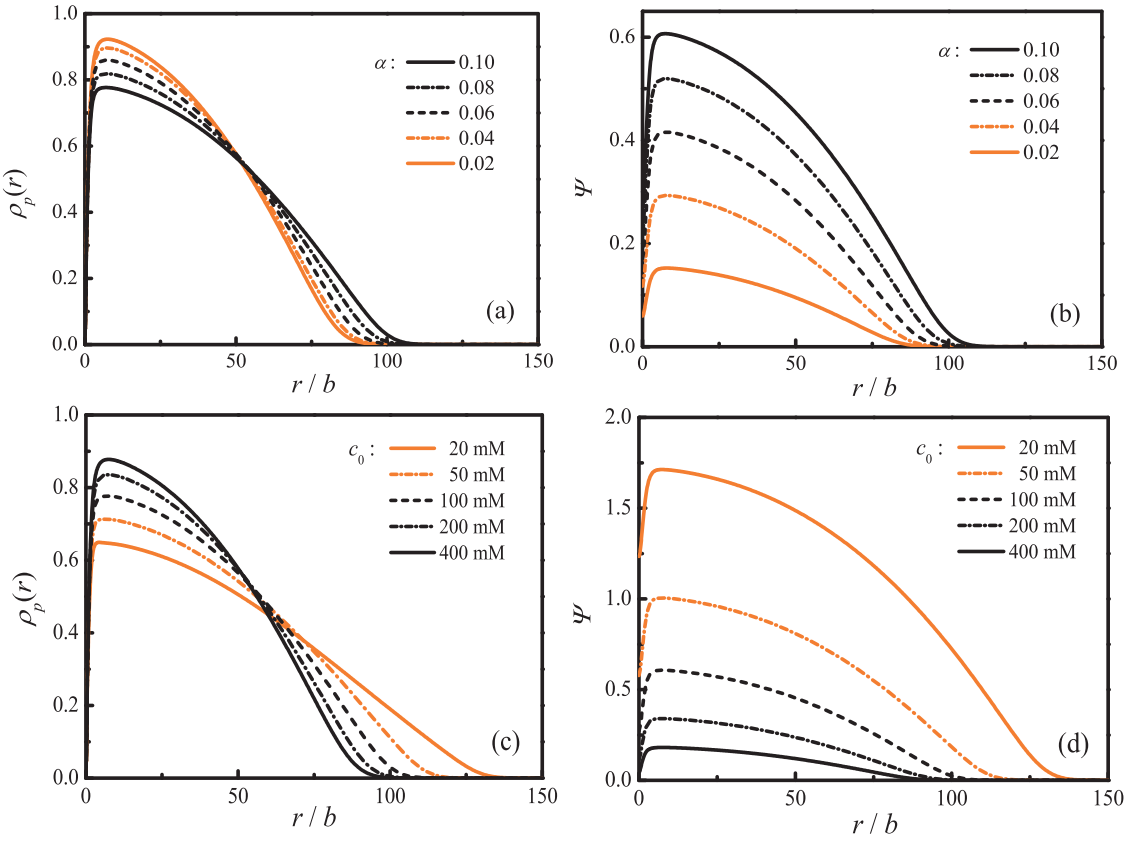

FIG. 1. (Color online) Structure of a polyelectrolyte brush grafted on a flat surface at different conditions. The parameters are fixed at $N = 500, \sigma = 0.1$, and $u_0 = 0.1$. Shown are spatial distributions of polymer segments and reduced electrostatic potential at (a) and (b) different fractions of charged segments ($\alpha = 0.02, 0.04, 0.06, 0.08,$ and 0.10) for a given salt concentration of $c_0 = 100$ mM and (c) and (d) different salt concentrations ($c_0 = 20, 50, 100, 200,$ and 400 mM) with a given fraction $\alpha = 0.10$. All lengths are expressed in units of b.

the calculations. Once all distributions are determined, the free energy can be obtained. By use of Eqs. (2) and (3), the elastic moduli from the charged polymer brush are deduced.

B. Results from numerical SCFT

In our previous work we used the SCFT to analyze systematically the effects of grafting density, chain length, and the interaction parameter of neutral polymer brushes on the bending modulus [27]. This article focuses on the contribution of the electrostatic interaction to curvature elasticity. The parameters related to charges, including the charge fraction α and salt concentration c_0, are investigated. We restrict our attention to some specified parameters. Namely, only long chains with chain length N varying from 100 to 500 are considered. The fraction of charge segments is set to be $0.01 \leqslant \alpha \leqslant 0.1$. The grafting density satisfies $\sigma \leqslant 0.1$. For simplicity, we set $l_B = b = 1$ nm. The excluded-volume parameter u_0 is fixed at 0 (θ solvent) or 0.1 (good solvent). With these parameters our method is applicable without taking into account the solvent explicitly. The salt concentration c_0 changes from 10 to 10000 mM. The system we deal with is a moderately grafted and weakly charged polymer brush and is comparable to the one in the SST.

We first investigate the structural properties of the polyelectrolyte brush. As shown in Fig. 1, one typical case displays the influence of the charge fraction and salt concentration on the structure of a planar brush. The parameters are fixed as $N = 500$, $u_0 = 0.1$, and $\sigma = 0.1$. Figures 1(a) and 1(b) give the segment density profiles and electrostatic potential distributions at different α, respectively. When polymer chains carry more charges, the electrostatic repulsion between segments is enhanced and the chains are forced to have more stretched conformations. Figures 1(c) and 1(d) show the effect of salt concentration when $\alpha = 0.1$. Apparently, high salt content leads to a high screening effect and reduces the electrostatic interaction. In this case, the segments tend to be distributed closer to that of a neutral polymer brush, i.e., the parabolic form. However, we also note that the electrostatic potential in the brush region varies abruptly, which means that the local electroneutrality approximation (constant potential in the brush) breaks down here.

In Fig. 2 we display our main SCFT results on the quantitative relation between the bending or Gaussian modulus and systematic parameters (α, σ, and N) for the fixed parameters of $c_0 = 100$ mM and $u_0 = 0.1$. After subtracting the contribution from the neutral polymer brush K_0, the remaining bending modulus induced by the electrostatic effect $K - K_0$ shows a good linear relation with respect to the variable of $(\alpha\sigma)^2$ for any different chain length N. Furthermore, we can put all the curves of different chain lengths into a unified function. Figure 2(b) shows $K - K_0$ as a function of a new combined variable $\alpha^2\sigma^2 N^{2.8}$ on a log-log scale. The good linear relationship over a broad range can be obtained by fitting and the slope is $\sim$1.0.

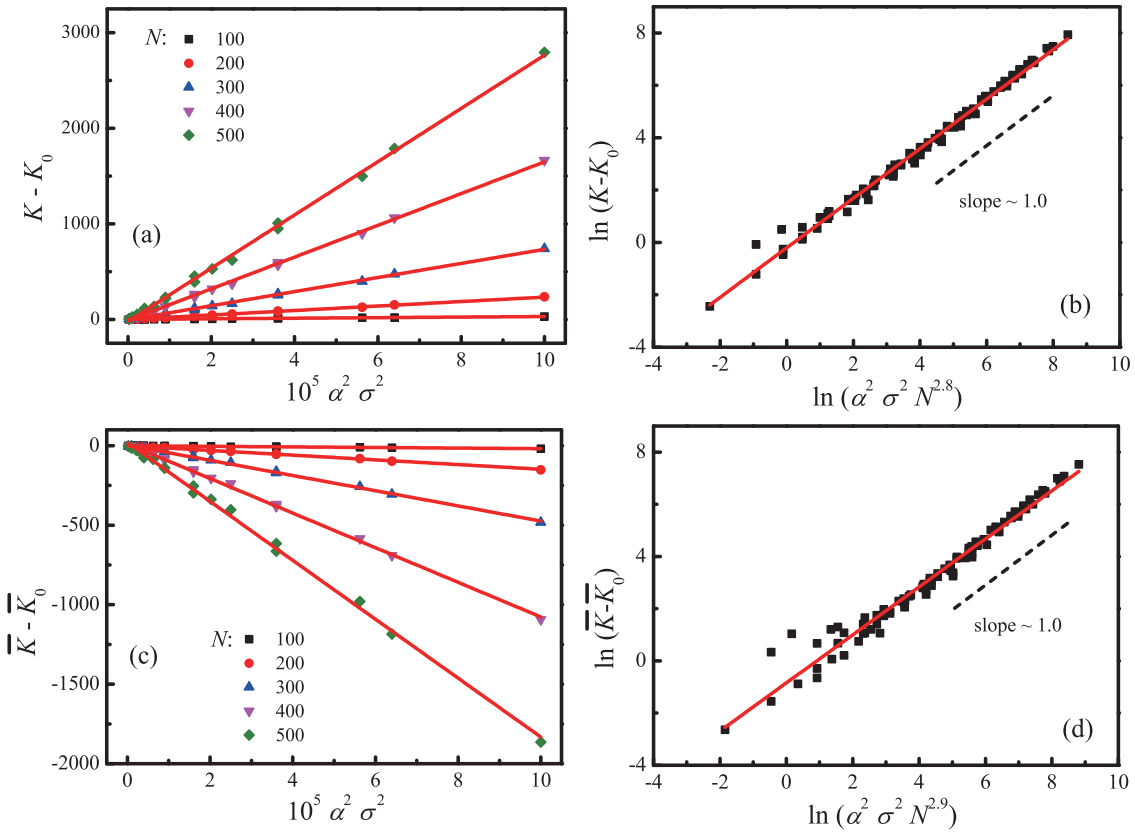

FIG. 2. (Color online) (a) Bending modulus K of a polyelectrolyte brush layer as a function of the fraction α and grafting density σ with $c_0 = 100$ mM and $u_0 = 0.1$. After subtracting the contribution from the neutral polymer brush K_0, the linear relationship is found between $K - K_0$ and $(\alpha\sigma)^2$. The charge fraction changes as $\alpha = 0.02, 0.04, 0.06, 0.08$, and 0.10, while the grafting density changes as $\sigma = 0.025, 0.050, 0.075$, and 0.100. The different chain lengths are displayed for $N = 100, 200, 300, 400$, and 500. (b) All data points in (a) are combined into a unified function of $\alpha^2\sigma^2N^{2.8}$. The linear fitting for $\ln(K - K_0)$ and $\ln(\alpha^2\sigma^2N^{2.8})$ produces a slope of $\sim$1.0. (c) The Gaussian modulus of the polyelectrolyte brush $\overline{K} - \overline{K}_0$ also has a linear relation with $(\alpha\sigma)^2$. All parameters are the same as in (a). (d) The absolute value of the Gaussian modulus $|\overline{K} - \overline{K}_0|$ is proportional to $\alpha^2\sigma^2N^{2.9}$, as shown on a log-log scale. All moduli are expressed in units of k_BT.

Based on these results, we believe that the relation between the bending modulus attributed to the electrostatic interactions and the related parameters satisfies the general rule

$$K - K_0 \approx A_B\alpha^2\sigma^2N^{2.8}, \tag{69}$$

where the prefactor A_B depends on the salt concentration c_0 and excluded-volume parameter u_0. For the case of Fig. 2(a) we have $A_B = 0.74$. In the Gaussian chain system without excluded-volume interactions ($u_0 = 0$), we get a different prefactor $A_B = 0.34$ at the same salt concentration $c_0 =$ 100 mM. Note that a few points in Fig. 2(b) deviate from the fitting line, which correspond to the cases where both the grafting density and charge fraction are very small. Since in this situation the total bending modulus K is close to the modulus K_0 of the neutral brush, the contribution from the charge effect is tiny and may have a large deviation. Similar scaling relations are found for the Gaussian modulus in Fig. 2(d), which scales as

$$\overline{K} - \overline{K}_0 \approx -A_G\alpha^2\sigma^2N^{2.9}, \tag{70}$$

where $A_G = 0.35$.

Next we study the effect of salt concentration on the bending modulus. In Fig. 3 we give the modulus $K - K_0$ induced by the electrostatic interaction as a function of salt concentration with $\sigma = 0.1$ on a log-log scale at different chain lengths [Fig. 3(a)] and at different charge fractions [Fig. 3(b)]. Two different regions can be distinguished for all curves. When the salt concentration is low ($c_0 < 100$ mM), the bending modulus decreases gradually with the decrease of c_0. However, for a relatively high value of c_0, the contribution from the charge effect is found to be inversely proportional to the salt concentration, i.e., $K - K_0 \sim c_0^{-1}$. This scaling relation holds over a broad range of parameter space. Similarly, the absolute value of the Gaussian modulus $|\bar{K} - \bar{K}_0|$ exhibits the same behavior as the bending modulus (data are not shown).

IV. DISCUSSION

The results from the SST [Eqs. (38) and (55)] and from the numerical SCFT calculation [Eqs. (69) and (70)] give quantitative predictions of the elastic moduli but with a different scaling law for the parameters. In order to get more insight into our results, we consider analytically a slightly bent polyelectrolyte brush in terms of scaling. Zhulina *et al.* [21] studied this system based on the assumption of the local electroneutrality approximation, which requires

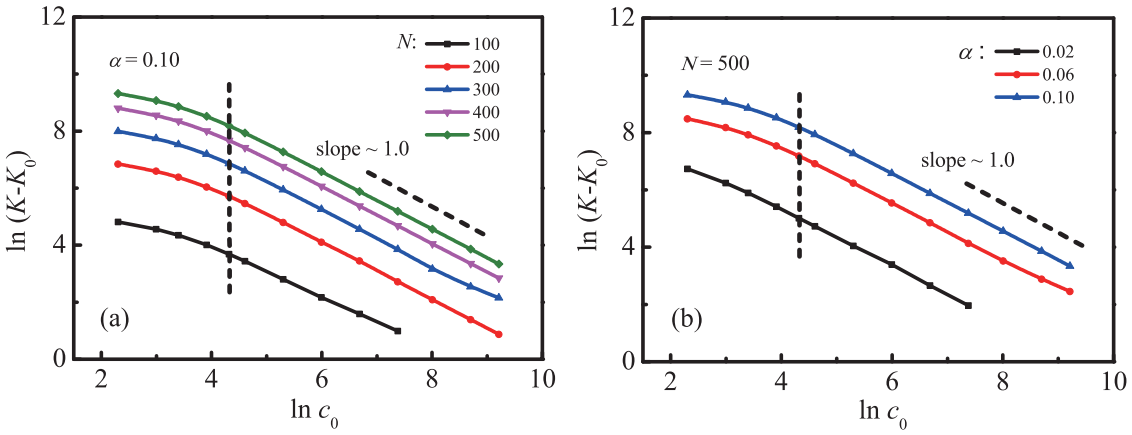

FIG. 3. (Color online) Bending modulus $K - K_0$ as a function of salt concentration on a log-log scale. The salt concentration c_0 changes from 10 to 10000 mM. The other parameters are $\sigma = 0.1$ and $u_0 = 0.1$. (a) The chain length changes as $N = 100$, 200, 300, 400, and 500 with a fixed charge fraction of $\alpha = 0.10$. (b) The charge fraction changes as $\alpha = 0.02$, 0.06, and 0.10 with a chain length of $N = 500$.

that the excess charge is always zero in the brush region, i.e., the electroneutrality condition is satisfied everywhere. When the salt concentration is high enough, the contribution of the electrostatic interaction to the free energy is given by $f_{\rm el} = \alpha^2\rho_p^2(r)/4c_0$ [$\alpha\rho_p(r) \ll c_0$] in the mean-field level. This term leads to an osmotic pressure in addition to that induced by the excluded-volume interaction and also gives an extra effective excluded volume to each segment $u_e = \alpha^2/4c_0$. In the limit $u_0 \ll u_e$, the contribution from the real excluded volume can be ignored and this situation corresponds to the so-called salted brush regime. The bending modulus from the charged brush is expressed as $K \sim N^3\sigma^{7/3}(\alpha^2/4c_0)^{4/3}$ by using the formula of the neutral brush [13,14]. This expression gives the same scaling dependence as our SST prediction (38) except for the prefactor. Thus our SST analysis under the Debye-Hückel approximation seems to represent a suitable modification to the local electroneurality approximation. The merit of our method consists in the prediction of quantified prefactors, which is the limitation of scaling arguments. Provided the maximum potential at the surface satisfies $\Psi(0) = A \leqslant 1$, the Debye-Hückel approximation is applicable. With $\kappa h_0 \gg 1$ this condition requires $A \approx Bh_0^2 \leqslant 1$. From Eq. (20) we find the condition ensuring the validity of our SST as

$$\frac{\alpha\sigma^2}{b^2c_0^2} \leqslant \frac{128}{27\pi^2}. \tag{71}$$

The numerical SCFT predicts a weaker dependence of elastic moduli on the charge fraction, salt concentration, and grafting density compared to the results from the SST. The main difference is that the SCFT adopts the nonlinear PB equation, while in the SST treatment the Debye-Hückel approximation (linearized PB equations) is used. In fact, this methodological difference indeed leads to the different dependence on the parameters. To illustrate this point we consider the case of a bare charged plane. On the basis of the PB equation, Lekkerkerker [45] derived the electrostatic contribution to the bending modulus of a plane with surface charge density σ_e as

$$K = \frac{1}{2\pi}\frac{k_BT}{l_B\kappa}\frac{(q-1)(q+2)}{(q+1)q}, \tag{72}$$

where $q = \sqrt{p^2+1}$ and $p = \frac{2\pi l_B|\sigma_e|}{\kappa}$. For a small surface charge density and a high salt concentration ($p \ll 1$), the bending modulus is reduced to the result based on the Debye-Hückel approximation [42]

$$K = \frac{k_BT3\pi l_B|\sigma_e|^2}{2\kappa^3}. \tag{73}$$

In contrast, when the surface charge density is large and the salt concentration is low ($p \gg 1$), the modulus can be expressed as

$$K = \frac{1}{2\pi}\frac{k_BT}{l_B\kappa}. \tag{74}$$

The Gaussian modulus induced by the electrostatic interaction has expressions similar to Eqs. (73) and (74) except for the numerical constants. Figure 4 shows the bending modulus K as a function of the surface charge density $|\sigma_e|$ (in arbitrary units) at a fixed κ from the nonlinear PB equation (72) (solid line) and the linearized PB equation (73) (dashed line). These two curves agree with each other very well when $|\sigma_e|$ is very small

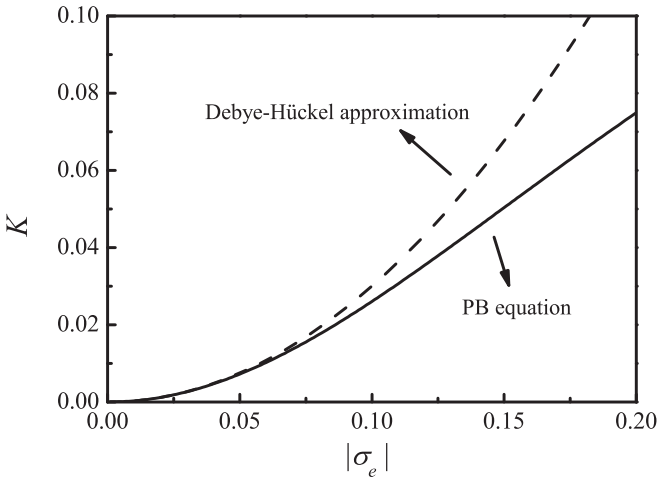

FIG. 4. Bending modulus K as a function of surface charge density $|\sigma_e|$. The solid line corresponds to the expression of the PB equation (72), while the dashed line corresponds to the linearized PB equation using the Debye-Hückel approximation (73).

($|\sigma_e| < 0.05$). However, at high surface charge density, the linearized PB equation obviously overestimates the electrostatic contribution to K compared to the nonlinear PB result. The grafted polyelectrolyte brush can be regarded as an analog to a charged flat surface with an effective surface charge density that is proportional to $\alpha\sigma N$ from a large length scale. Therefore, for the same reason, in our case the SST gives an effect of the parameters α, σ, and N on the bending modulus stronger than the SCFT calculation since we have to introduce the Debye-Hückel approximation in the analytical SST. Another possible reason for the difference between two methods comes from the neglect of the polymer entropy in the SST approach, including the entropy associated with free end distribution and entropy loss due to the impenetrable membrane. These entropic terms have a significant effect on the brush profile, the charge distribution, and the electrostatic energy if the parameter charactering the degree of stretching β is small [52]. In our system, these entropic contributions are not expected to be a dominant factor since β is large enough here. At the same time, the electrostatic force results in the further stretching of chains, which is favorable to validate the SST treatment.

It is worthwhile to make a further comparison between the polyelectrolyte brush and a bare charged surface. Introducing the notation $\sigma_{\text{eff}} = \alpha\sigma N$, which represents the number of charges per unit area carried by the polymer brush, σ_{eff} is equal to the effective surface charge density if all charges in the brush are collapsed onto the flat surface. Equation (69) from the SCFT treatment can be rewritten as

$$K - K_0 \sim (\alpha\sigma N)^2 N^{0.8} \sim \sigma_{\text{eff}}^2 N^{0.8}. \tag{75}$$

The Gaussian modulus has the same expression as $\overline{K} - \overline{K}_0 \sim \sigma_{\text{eff}}^2 N^{0.9}$. Consequently, the bending modulus calculated by the numerical SCFT is also proportional to the square of the effective surface charge density, which is in agreement with the result of a bare charged plane in the limit $p \ll 1$. It is noted that we have an extra term $N^{0.8}$ in Eq. (75), which can be regarded as a correction to a charged flat surface due to the presence of a polymer brush. This term characterizes a unique effect when the surface is covered by a soft shell of polymers. However, it is not clear about the inherent meaning of the exponent 0.8.

The effect of added salts reveals more details on the difference between a bare charged surface and a charged polymer brush. Based on Eqs. (73) and (74), the bare charged surface has the bending modulus scaling as $K, \overline{K} \sim c_0^{-3/2}$ at high salt concentration and $K, \overline{K} \sim c_0^{-1/2}$ at low salt concentration (note that $\kappa^2 \sim c_0$). When the salt concentration c_0 is extremely small, the screening effect of mobile ions is weak and the potential Ψ is relatively large. One may expect that a charged brush (the Pincus brush regime without added salt) behaves similarly to a bare charged plane as $K, \overline{K} \sim c_0^{-1/2}$ for $\kappa^{-1} \gg h_0$ [28]. However, in this case our analytical SST is not applicable due to the strong electrostatic potential. The results from the numerical SCFT at low salt concentrations do not follow a simple scaling relation between the modulus and c_0. Most probably the low salt concentrations we used here do not satisfy the condition $p \gg 1$. At very high salt concentration c_0, the SCFT gives $K, \overline{K} \sim c_0^{-1}$, while the SST predicts $K, \overline{K} \sim c_0^{-4/3}$. The absolute values of these exponents are smaller than the value of $3/2$ for a bare charged surface. The weaker dependence on salt concentration reveals the essential difference between a polyelectrolyte brush and a bare charged surface. Namely, the charges loaded on polymers spread across the whole brush zone. These polymer charges and mobile ions can adjust their positions in the three-dimensional space during the bending process. Thus the charged polymer brush system has more degrees of freedom than the bare charged surface. The redistribution of all charged particles leads to a weaker screening effect of added salts on the repulsive electrostatic force acting on the surface.

V. CONCLUSION

In this paper we calculated the elastic constants (bending modulus and Gaussian modulus) induced by a polyelectrolyte brush monolayer grafted on a solid surface. Both the analytical method based on the SST and the numerical calculations based on the SCFT were applied. We focused on the scaling relation between elastic moduli and systematic parameters for the charge effect (charge fraction α and salt concentration c_0) and compared results from the two methods. In the analytical treatment, adopting a Gaussian chain model, based on a parabolic external potential assumption within the SST framework and a Debye-Hückel approximation for the PB equation, we derived the structure and the free energy of a brush in flat, cylindrical, and spherical coordinates, respectively. Expanding the free energy as a power series of the curvature in the cases of the cylindrical and the spherical brushes, we obtained analytical expressions for elastic moduli. In the SCFT treatment, the nonideal chain model was investigated by explicitly taking into account the excluded-volume interaction. In our calculation, the chain length was relatively long while both the charge fraction and grafting density were low. The inner structure and the free energy were numerically calculated in different coordinates and the moduli were obtained by fitting. It was found that the elastic moduli induced by the electrostatic interaction (after subtracting the contribution of the neutral polymer brush) scale as $\alpha^2\sigma^2$ and are inversely proportional to the salt concentration c_0 when the salt concentration is high enough. A simple scaling argument based on the local electroneutrality approximation gave results similar to those from our SST, indicating the validity of our analytical SST in this system. We also found that the SST result for the scaling exponents with respect to systematic parameters is larger than that from the SCFT. This was attributed to the linearization of the PB equation in the analytical derivation, rendering the analytical SST applicable in a limited parameter space.

Furthermore, we compared the grafted polyelectrolyte brush system with a bare charged surface and found some common features about their contributions to the surface modulus induced by the electrostatic interaction. However, the different scaling exponents of elastic moduli with respect to chain length N and salt concentration c_0 revealed the special role played by polymer chains in determining the modulus.

In summary, we have investigated systematically the elastic moduli induced by a polyelectrolyte brush and obtained several important scaling relations. These findings provide a deep understanding of the polyelectrolyte brush, but we need to seek further experiments to confirm the predictions. It should

be noted that the correlational electrostatic contribution is not introduced here, which is very important in polyelectrolyte solutions [53,54]. The rational consideration of the electrostatic correlation effect of a charged brush involves in complicated calculations since the complex coupling between charges and polymer chains is anisotropic for the brush. This issue in left to future investigation.

ACKNOWLEDGMENTS

We thank Professor David Andleman and Professor Dadong Yan for helpful discussions. This work was supported by the National Natural Science Foundation of China (Grants No. 21474005, No. 21104094, and No. 21474002). B.M. acknowledges support from the Youth Innovation Promotion Association, CAS.

[1] S. A. Safran, Curvature elasticity of thin films, Adv. Phys. **48**, 395 (1999).
[2] W. Helfrich, Elastic properties of lipid bilayers: Theory and possible experiments, Z. Naturforsch. **28c**, 693 (1973).
[3] M. Rovira-Bru, D. H. Thompson, and I. Szleifer, Size and structure of spontaneously forming liposomes in lipid/PEG-lipid mixtures, Biophys. J. **83**, 2419 (2002).
[4] I. Tsafrir, Y. Caspi, M.-A. Guedeau-Boudeville, T. Arzi, and J. Stavans, Budding and tubulation in highly oblate vesicles by anchored amphiphilic molecules, Phys. Rev. Lett. **91**, 138102 (2003).
[5] F. Campelo and A. Hernández-Machado, Polymer-induced tubulation in lipid vesicles, Phys. Rev. Lett. **100**, 158103 (2008).
[6] D. Marsh, Elastic constants of polymer-grafted lipid membranes, Biophys. J. **81**, 2154 (2001).
[7] D. Marsh, R. Bartucci, and L. Sportelli, Lipid membranes with grafted polymers: physicochemical aspects, Biochim. Biophys. Acta **1615**, 33 (2003).
[8] Z. G. Wang and S. A. Safran, Equilibrium emulsification of polymer blends by diblock copolymers, J. Phys. **51**, 185 (1990).
[9] Y. Lauw, F. A. M. Leermakers, M. A. Cohen Stuart, O. V. Borisov, and E. B. Zhulina, Coexistence of crew-cut and starlike spherical micelles composed of copolymers with an annealed polyelectrolyte block, Macromolecules **39**, 3628 (2006).
[10] L. Xu, Z. C. Zhu, O. V. Borisov, E. B. Zhulina, and S. A. Sukhishvili, *p*H-triggered block copolymer micelle-to-micelle phase transition, Phys. Rev. Lett. **103**, 118301 (2009).
[11] M. W. Matsen, Elastic properties of a diblock copolymer monolayer and their relevance to bicontinuous microemulsion, J. Chem. Phys. **110**, 4658 (1999).
[12] I. Szleifer, D. Kramer, A. Benshaul, W. M. Gelbart, and S. A. Safran, Molecular theory of curvature elasticity in surfactant films, J. Chem. Phys. **92**, 6800 (1990).
[13] Z. G. Wang and S. A. Safran, Curvature elasticity of diblock copolymer monolayers, J. Chem. Phys. **94**, 679 (1991).
[14] S. T. Milner and T. A. Witten, Bending moduli of polymeric surfactant interfaces, J. Phys. **49**, 1951 (1988).
[15] L. Leibler, Emulsifying effects of block copolymers in incompatible polymer blends, Makromol. Chem. Macromol. Symp. **16**, 1 (1988).
[16] R. S. Cantor, Statistical thermodynamics of curvature elasticity in surfactant monolayer films: A molecular approach, J. Chem. Phys. **99**, 7124 (1993).
[17] F. Clément and J.-F. Joanny, Curvature elasticity of an adsorbed polymer layer, J. Phys. II **7**, 973 (1997).
[18] M. Müller and G. Gompper, Elastic properties of polymer interfaces: Aggregation of pure diblock, mixed diblock, and triblock copolymers, Phys. Rev. E **66**, 041805 (2002).
[19] K. Chang and D. C. Morse, Diblock copolymer surfactants in immiscible homopolymer blends: Interfacial bending elasticity, Macromolecules **39**, 7397 (2006).
[20] C. Hiergeist and R. Lipowsky, Elastic properties of polymer decorated membranes, J. Phys. II **6**, 1465 (1996).
[21] E. B. Zhulina, T. M. Birshtein, and O. V. Borisov, Curved polymer and polyelectrolyte brushes beyond the Daoud-Cotton model, Eur. Phys. J. E **20**, 243 (2006).
[22] I. Szleifer, O. V. Gerasimov, and D. H. Thompson, Spontaneous liposome formation induced by grafted poly(ethylene oxide) layers: Theoretical prediction and experimental verification, Proc. Natl. Acad. Sci. USA **95**, 1032 (1998).
[23] P. A. Barneveld, D. E. Hesselink, F. A. M. Leermakers, J. Lyklema, and J. M. H. M. Scheutjens, Bending moduli and spontaneous curvature. 2. Bilayers and monolayers of pure and mixed ionic surfactants, Langmuir **10**, 1084 (1994).
[24] T. M. Birshtein, P. A. Lakovlev, V. M. Arnoskov, F. A. M. Leermakers, E. B. Zhulina, and O. V. Borisov, On the curvature energy of a thin membrane decorated by polymer brushes, Macromolecules **41**, 478 (2008).
[25] S. D. Stoyanov, V. N. Paunov, H. Kuhn, and H. Rehage, A general method for calculating bending moduli and spontaneous curvature of polymer brushes in terms of local density functional theory, Macromolecules **36**, 5032 (2003).
[26] M. Laradji, Elasticity of polymer-anchored membranes, Europhys. Lett. **60**, 594 (2002).
[27] Z. Lei, S. Yang, and E.-Q. Chen, Membrane rigidity induced by grafted polymer brush, Soft Matter **11**, 1376 (2015).
[28] P. Pincus, Colloid stabilization with grafted polyelectrolytes, Macromolecules **24**, 2912 (1991).
[29] O. V. Borisov, E. B. Zhulina, and T. M. Birshtein, Diagram of the states of a grafted polyelectrolyte layer, Macromolecules **27**, 4795 (1994).
[30] R. S. Ross and P. Pincus, The polyelectrolyte brush: poor solvent, Macromolecules **25**, 2177 (1992).
[31] E. B. Zhulina, O. V. Borisov, and T. M. Birshtein, Structure of grafted polyelectrolyte layer, J. Phys. II **2**, 63 (1992).
[32] R. Israels, F. A. M. Leermakers, G. J. Fleer, and E. B. Zhulina, Charged polymeric brushes—Structure and scaling relations, Macromolecules **27**, 3249 (1994).
[33] E. B. Zhulina and O. V. Borisov, Structure and interaction of weakly charged polyelectrolyte brushes: Self-consistent field theory, J. Chem. Phys. **107**, 5952 (1997).
[34] E. B. Zhulina, J. K. Wolterink, and O. V. Borisov, Screening effects in a polyelectrolyte brush: Self-consistent-field theory, Macromolecules **33**, 4945 (2000).
[35] M. W. Matsen, Effect of salt on the compression of polyelectrolyte brushes in a theta solvent, Eur. Phys. J. E **35**, 13 (2012).

[36] L. Chen, H. Merlitz, S.-z. He, C.-X. Wu, and J.-U. Sommer, Polyelectrolyte brushes: Debye approximation and mean-field theory, Macromolecules **44**, 3109 (2011).

[37] F. Vongoeler and M. Muthukumar, Polyelectrolyte brush density profiles, Macromolecules **28**, 6608 (1995).

[38] K. N. Witte, S. Kim, and Y.-Y. Won, Self-consistent field theory study of the effect of grafting density on the height of a weak polyelectrolyte brush, J. Phys. Chem. B **113**, 11076 (2009).

[39] C. Seidel, Strongly stretched polyelectrolyte brushes, Macromolecules **36**, 2536 (2003).

[40] A. Naji, C. Seidel, and R. R. Netz, Theoretical approaches to neutral and charged polymer brushes, Adv. Polym. Sci. **198**, 149 (2006).

[41] J. Klein Wolterink, F. A. M. Leermakers, G. J. Fleer, L. K. Koopal, E. B. Zhulina, and O. V. Borisov, Screening in solutions of star-branched polyelectrolytes, Macromolecules **32**, 2365 (1999).

[42] M. Winterhalter and W. Helfrich, Effect of surface-charge on the curvature elasticity of membranes, J. Phys. Chem. **92**, 6865 (1988).

[43] A. Fogden and B. W. Ninham, The bending modulus of ionic lamellar phases, Langmuir **7**, 590 (1991).

[44] J. L. Harden, C. Marques, J. F. Joanny, and D. Andelman, Membrane curvature elasticity in weakly charged lamellar phases, Langmuir **8**, 1170 (1992).

[45] H. N. W. Lekkerkerker, Contribution of the electric double layer to the curvature elasticity of charged amphiphilic monolayers, Physica A **159**, 319 (1989).

[46] A. Fogden and B. W. Ninham, Electrostatics of curved fluid membranes: The interplay of direct interactions and fluctuations in charged lamellar phases, Adv. Colloid Interface Sci. **83**, 85 (1999).

[47] A. Victorov, Curvature elasticity of a weak polyelectrolyte brush and shape transitions in assemblies of amphiphilic diblock copolymers, Soft Matter **8**, 5513 (2012).

[48] M. Manghi, M. Aubouy, C. Gay, and C. Ligoure, Inwardly curved polymer brushes: concave is not like convex, Eur. Phys. J. E **5**, 519 (2001).

[49] A. Shafir and D. Andelman, Bending moduli of charged membranes immersed in polyelectrolyte solutions, Soft Matter **3**, 644 (2007).

[50] A. N. Semenov, Contribution to the theory of microphase layering in block-copolymer melts, Sov. Phys. JETP **61**, 733 (1985).

[51] E. B. Zhulina, O. V. Borisov, V. A. Pryamitsyn, and T. M. Birshtein, Coil-globule type transitions in polymers. 1. Collapse of layers of grafted polymer chains, Macromolecules **24**, 140 (1991).

[52] R. R. Netz and M. Schick, Polymer brushes: From self-consistent field theory to classical theory, Macromolecules **31**, 5105 (1998).

[53] V. Y. Borue and I. Y. Erukhimovich, A statistical theory of weakly charged polyelectrolytes: Fluctuations, equation of state and microphase separation, Macromolecules **21**, 3240 (1988).

[54] V. Y. Borue and I. Y. Erukhimovich, A statistical theory of globular polyelectrolyte complexes, Macromolecules **23**, 3625 (1990).